Robust Digital Control for Interleaved PFC Boost Converters Using an Approximate 2DOF Current Controller

Yuto Adachi*, **Kohji Higuchi***[1],
Tomoaki Sato**, Non-members, and **Kosin Chamnongthai*****, Member

ABSTRACT

In recent years, improving power factor and reducing harmonics distortion of power supply used in electrical instruments are needed. In general, a current conduction mode boost converter is used for an active PFC (Power Factor Correction). Especially, an interleaved PFC boost converter is used to make a size compact, make an efficiency high and make a noise low. In this paper, the design method using an Approximate 2-degree-of-freedom (A2DOF) controller for a current control system and using a digital PI controller for a voltage control system is proposed. The digital PI controller is designed to enlarge the control bandwidth of the voltage control system. By this design method, the power factor can be improved more, the input current distortion can be made smaller and the output voltage regulation can also be suppressed smaller. These controllers are actually implemented on a micro- processor and are connected to the PFC converter. Experimental studies demonstrate that the combination of the digital A2DOF current controller and the digital PI voltage controller are effective. And it is shown that this combination is better than the one of usual phase lead-lag compensation controllers in the power factor, the input current distortion and the output voltage regulation.

Keywords: Interleaved PFC, Boost converter, Digital robust control, A2DOF, Micro-processor.

1. INTRODUCTION

In recent years, improving power factor and reducing harmonics of power supply used in electrical instruments such as servers are needed. A passive filter and an active filter in AC lines are used for improving the power factor and reducing the harmonics [1-2]. Generally a current conduction mode boost converter is used for an active PFC (Power Factor Correction) in electrical instruments. Especially, an interleaved PFC boost converter is used in order to make a size compact, make an efficiency high and make a noise low.

In the PFC boost converter, if a duty ratio, a load resistance and an input voltage are changed, the dynamic characteristics are varied greatly, that is, the PFC converter has non-linear characteristics. In many applications of the interleaved PFC converters, loads cannot be specified in advance, i.e., their amplitudes are suddenly changed from the zero to the maximum rating. This is the prime reason of difficulty of controlling the PFC boost converter.

Usually, a conventional PI controller or an analog IC controller designed to an approximated linear controlled object at one operating point is used for the PFC converter, but the control performances are not so good because the input current distortion and the output voltage regulation are comparatively large [3-8]. Authors proposed an Approximate 2-degree-of-freedom (A2DOF) control method of buck converters previously [9-10]. Moreover, this method was applied to PFC boost converters, and the digital control method using a A2DOF current controller and a A2DOF voltage controller was proposed [11-12]. In this design method, first, when the current A2DOF controller is designed, the zeros of the controlled object near 1 in the unit circle is canceled by one of the poles in the model matching system in order to eliminate the differentiation characteristics. Next, the pole cancelled is used as the dominant pole for designing the voltage A2DOF controller. The zeros of the interleaved PFC boost converter (controlled object) is very close to 1. Then if the cancellation pole is used as the dominant pole for the voltage A2DOF controller, the output voltage response is very slow, and the voltage regulation gets very bad. So this type voltage A2DOF controller cannot apply to the interleaved PFC boost converter.

In this paper, the digital control method using the A2DOF current controller and the PI voltage controller is proposed. The digital PI controller is designed to enlarge the control bandwidth of the voltage control system, keeping the characteristics of the current control system. By this design method, the power factor can be improved more, the input current distortion can be made smaller and the output volt-

Manuscript received on January 13, 2013 ; revised on February 24, 2013.
* The authors are with The University of Electro-Communications, Japan, E-mail: higuchi@ee.uec.ac.jp[1]
** The author is with C&C SYSTEMS CENTER Hirosaki University, Japan
*** The author is with King Mongkut's University of Technology Thonburi, Thailand.

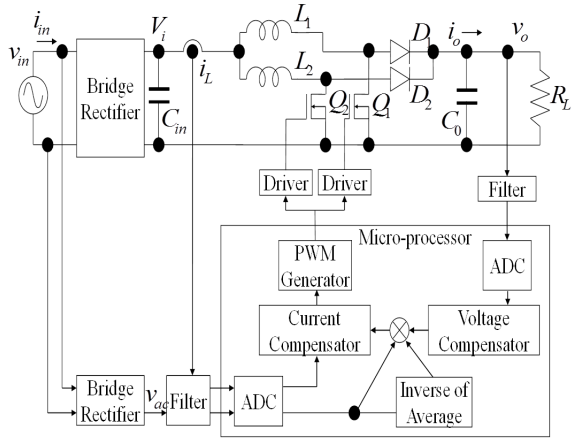

Fig. 1: *Interleaved PFC boost converter.*

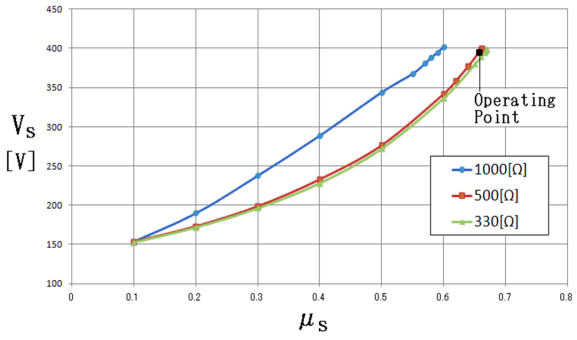

Fig. 2: *The static characteristics of μ_s to V_s.*

age regulation can also be suppressed smaller than the usual lead-lag control method. These controllers are actually implemented on a micro-processor and is connected to the PFC converter. Experimental studies demonstrate that the combination of the digital A2DOF current controller and digital PI voltage controller are effective. And it is shown that this combination is better than the one of the phase lead-lag controllers in the power factor, the input current distortion and the output voltage regulation.

2. INTERLEAVEDD PFC BOOST CONVERTER

The interleaved PFC boost converter shown in Fig. 1 is manufactured. Fig.1, v_{in} is an input AC voltage, i_{in} is an input AC current, C_{in} is a smoothing capacitor, V_i is a rectifying and smoothing input voltage, Q_1 and Q_2 are MOSFETs or IGBTs, L_1 and L_2 are interleaved boost inductances, D_1 and D_2 are interleaved boost diodes, C_0 is an output capacitor, R_L is an output load resistance, i_L is a sum of the inductor currents, v_{ac} is an absolute value of the input AC voltage and v_o is an output voltage. The inductor current i_L is controlled to follow the rectified input voltage v_{ac} for improving the power factor, reducing the harmonics and stabilizing the output voltage. Here V_{in}=100[V_{AC}], V_i=140[V_{DC}], v_o = 395[V_{DC}], L_1= L_2=400[μH], C_0=440[μF], the switching frequency is f_{sw}=35[kHz]. the sampling frequency is f_s=70[kHz].

Using the state-space averaging method, the state equation of the interleaved boost converter becomes as follows [13]:

$$\frac{d}{dt}\begin{bmatrix} i_0 \\ v_0 \end{bmatrix} = \frac{d}{dt}\begin{bmatrix} \frac{-R_0}{L_0} & \frac{-1}{L_0} \\ \frac{1}{C_0} & \frac{-1}{R_L C_0} \end{bmatrix}\begin{bmatrix} i_0 \\ v_0 \end{bmatrix} + \begin{bmatrix} \frac{V_i}{L_0} \\ 0 \end{bmatrix} + \left\{ v_0 \begin{bmatrix} \frac{1}{L_0} \\ 0 \end{bmatrix} + i_0 \begin{bmatrix} 0 \\ \frac{-1}{C_0} \end{bmatrix} \right\} u \tag{1}$$

Here μ is a duty ratio. When the sum of inductor currents is controlled as 1-phase, i_o is i_L , R_0 is $R_1R_2/(R_1+R_2)$ and L_0 is $L_1L_2/(L_1+L_2)$ (R_1 and R_2 are equivalent series resistances of inductances L_1 and L_2, respectively). The PFC boost converter has non-linear characteristics because this equation has the product of the state variable v_o, i_o and the duty ratio Îij.

At some operating point of eq. (1), let v_o, i_L and μ, be V_s, I_s and μ_s, respectively. Then the average of the output voltage V_s and the inductor current Is at the operating point become as follows:

$$\begin{aligned} V_s &= \frac{1}{1+\frac{1}{(1+\mu_s)^2}\frac{R_0}{R_L}}\frac{1}{1-\mu_s}V_i \\ I_s &= \frac{1}{R_L}\frac{V_s}{1-\mu_s} \end{aligned} \tag{2}$$

The actual measurement results of the static characteristics of μ_s to V_s are shown in Fig.2. In Fig.2, it turns out that the PFC boost converter is a non-linear system. The static characteristics of the PFC boost converter are changed greatly with load resistances, and it influences the dynamic characteristics of the PFC converter. In addition, the static characteristics will be changed with input voltage variation

The linear approximate state equation of the PFC boost converter using small perturbations $\Delta i_L = i_L - I_s$, $\Delta v_o = v_o - V_s$ and $\Delta\mu = \mu - \mu_s$ is as follows [13]:

$$\begin{aligned} \dot{x}(t) &= A_c x(t) + B_c u(t) \\ y(t) &= C_c x(t) \end{aligned} \tag{3}$$

where

$$A_c = \begin{bmatrix} \frac{-R_0}{L_0} & \frac{-(1-\mu_s)}{L_0} \\ \frac{-(1-\mu_s)}{C_0} & \frac{-1}{R_L C_0} \end{bmatrix},\ B_c = \begin{bmatrix} \frac{V_s}{L_0} \\ \frac{-I_s}{C_0} \end{bmatrix}$$

$$x(t) = \begin{bmatrix} \Delta i_L(t) \\ \Delta v_0(t) \end{bmatrix}, u(t) = \Delta\mu(t), y = \begin{bmatrix} y_i \\ y_v \end{bmatrix}, C_c = \begin{bmatrix} 1 \\ 0 \end{bmatrix}$$

From this equation, matrix A_c and B_c of the PFC boost converter depend on the duty ratio μ_s. Therefore, the PFC boost converter response will be changed depending on the operating point and the other parameter variation. The changes of the load ${}_RL$, the duty ratio μ_s, the output voltage V_s and the inductor current Is in the controlled object are con-

sidered as parameter changes in eq. (1). Such the parameter changes can be replaced with the equivalent disturbances inputted to the input and the output of the controlled object. Therefore, what is necessary is just to constitute the control systems whose pulse transfer functions from the equivalent disturbances to the output y become as small as possible in their amplitudes, in order to robustize or suppress the influence of these parameter changes.

3. DESIGN OF DIGITAL CONTROLLERS

3.1 Discretization of controlled object

The continuous system of eq. (1) is transformed into the discrete system as follows:

$$\begin{aligned} x_d(k+1) &= A_d x_d(k) + B_d u(k) \\ y(k) &= C_d x_d(k) \end{aligned} \tag{4}$$

where
$A_d = \left[e^{A_c T}\right], B_d = \left[\int_0^T e^{A_c T} B_c d\tau\right], C_d = C_c$
Here, in order to compensate the delay time by A/D conversion time and micro-processor operation time etc., one delay (state $\zeta 1$) is introduced to the input of the controlled object. Then the state-space equation is described as follows:

$$\begin{aligned} x_{dt}(k+1) &= A_{dt} x_{dt}(k) + B_{dt} v(k) \\ y(k) &= C_{dt} x_{dt}(k) \end{aligned} \tag{5}$$

where

$$A_{dt} = \begin{bmatrix} e^{A_c T_s} & e^{A_c (T_s - L_d)} \int_0^{L_d} e_c^A \tau B_c d\tau \\ 0 & 0 \end{bmatrix}$$

$$B_{dt} = \begin{bmatrix} \int_0^{T_s - L_d} e^{A_c \tau} B_c d\tau \\ 1 \end{bmatrix} \quad x_{dt}(k) = \begin{bmatrix} x(k) \\ \zeta_1(k) \end{bmatrix}$$

$$C_{dt} = \begin{bmatrix} C_c & 0 \end{bmatrix} = \begin{bmatrix} 1 & 0 & 0 \end{bmatrix}$$

3.2 A2DOF digital current controller

The transfer function from the reference input $r_i^{'}$ to the output y_i is specified as follows:

$$\begin{aligned} W_{r_i' y i}(z) = & \frac{(1+H_1)}{(z+H_1)} \frac{(1+H_2)}{(z+H_2)} \frac{(1+H_3)}{(z+H_3)} \\ & \times \frac{(z-n_{1i})}{(1-n_{1i})} \frac{(z-n_{2i})}{(1-n_{2i})} \end{aligned} \tag{6}$$

Here H_i, i=1,2,3 are the specified arbitrary parameters, n_{1i} and n_{2i} are the zeros of the discrete-time controlled object. This target characteristic $W_{r_i' y i}$ is realizable by constituting the model matching system shown in Fig.3 using the following state feedback to the controlled object (5).

$$v = -F x_{dt} + G_i r_i^{'} \tag{7}$$

Here F = $[f1 f2 f3]$ and G_i are selected suitably. In Fig. 3, q_v and q_{yi} are the equivalent disturbances

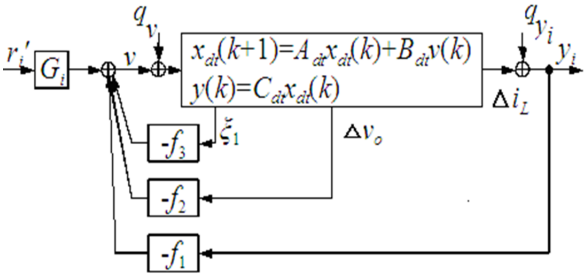

Fig.3: *Model matching system using state feedback.*

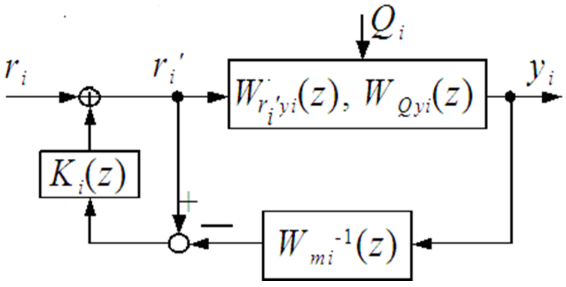

Fig.4: *System reconstituted with inverse system and filter.*

with which the parameter changes of the controlled object are replaced.

It shall be specified that the relation of H_1 and H_3 become $|H1| \gg |H3|$ and $H_2 = n_{1i}$. Then $W_{r_i' y i}$ can be approximated to the following first-order discrete-time model:

$$W_{r_i' y i}(z) \approx W_{mi}(z) = \frac{1+H_1}{z+H_1} \tag{8}$$

The transfer function $W_{Qyi}(z)$ between the equivalent disturbance $Qi = [q_v \quad q_{yi}]^T$ to y_i of the system in Fig.3 is defined as

$$W_{Qyi}(z) = \begin{bmatrix} W_{q_v y_i}(z) & W_{q_{yi} y_i}(z) \end{bmatrix} \tag{9}$$

The system added the inverse system and the filter to the system in Fig.3 is constituted as shown in Fig.4. In Fig.4, the transfer function Ki(z) is as follows:

$$K_i(z) = \frac{k_{zi}}{z - 1 + k_{zi}} \tag{10}$$

The transfer functions between $r_i - y_i, q_v - y_i$ and $q_{yi} - y_i$ of the system in Fig.4 are given by

$$y_i = \frac{1+H_1}{z+H_1} \frac{z-1+k_{zi}}{z-1+k_{zi} W_{si}(z)} W_{si}(z) r_i \tag{11}$$

$$y_i = \frac{z-1+k_{zi}}{z-1+k_{zi}} \frac{z-1+k_{zi}}{z-1+k_{zi} W_{si}(z)} W_{Qyi}(z) Q_i \tag{12}$$

where

$$W_{si}(z) = \frac{(1+H_3)}{(z+H_3)} \frac{(z-n_{1i})}{(1-n_{1i})}$$

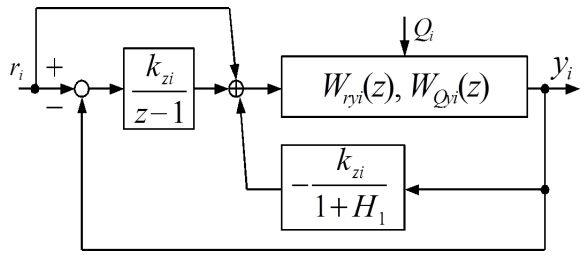

Fig.5: *Equivalent transformation of the robust digital controller.*

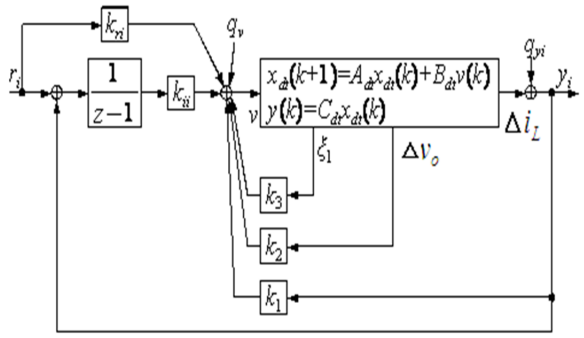

Fig.6: *Approximate 2DOF digital integral type current control system.*

Here, if $W_{si}(z) \approx 1$ within the bandwidth needed, then eq. (11) and eq. (12) are approximated as follows, respectively:

$$y_i \approx \frac{1+H_1}{z+H_1} r_i \tag{13}$$

$$y_i \approx \frac{z-1}{z-1+k_{zi}} W_{Qyi}(z) Q_i \tag{14}$$

From eq. (13) and (14), it turns out that the characteristics from r_i to y_i can be specified with H_1 and the characteristics from Q_i to y_i can be specified with k_{zi} independently. That is, the system in Fig.4 is an A2DOF system, and its sensitivity against disturbances becomes lower with the increase of k_{zi}. If the controller in Fig.4 is transformed equivalently, we obtain Fig.5. Then, substituting the system of Fig. 3 to Fig. 5, the A2DOF digital integral type control system will be obtained as shown in Fig.6. In Fig.6, the parameters of the controller are as follows:

$$\begin{aligned} &k_1 = -f_1 - \frac{Gk_{zi}}{1+H_1}, \quad k_2 = -f_2 \\ &k_3 = -f_3, \quad k_{ii} = G_i k_{zi}, \quad k_{ri} = G_i \end{aligned} \tag{15}$$

3.3 PI digital voltage controller

The multiplier is added to the reference input r_i of the current control system. Let the inputs of the multiplier be v_{ac} and u_v as shown in Fig.7. The v_{ac} is the absolute value of the input voltage vin, and u_v

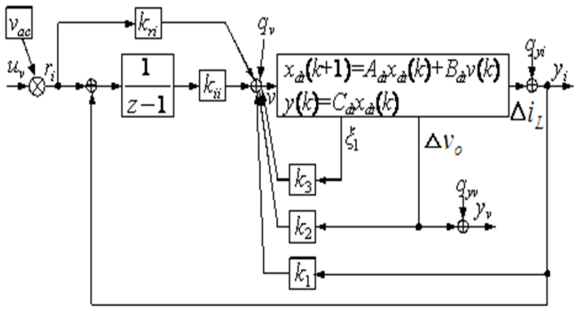

Fig.7: *Current control system added multiplier.*

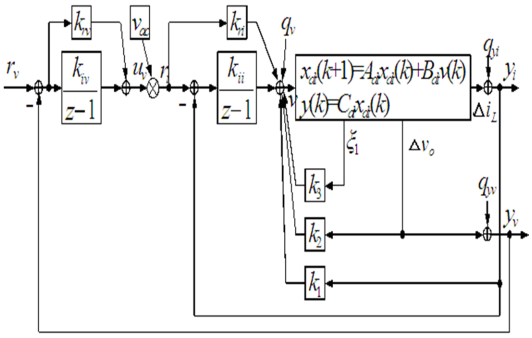

Fig.8: *Digital robust control system including the A2DOF current controller and the PI voltage controller.*

is a new input. This addition is added for making the inductor current i_L follow the AC voltage v_{ac}.

Next, the digital PI voltage controller is added to the input of Fig.7. Then the digital robust control system including the A2DOF current controller and the PI voltage controller is obtained as shown in Fig.8.

4. EXPERIMENTAL STUDIES

Experimental setup system shown in Fig. 9 is manufactured. A micro-controller (RX) from Renesas Electronics is used for the digital controller. The digital A2DOF current controller and the PI voltage controller were implemented on 1 micro-processor.

The A2DOF current control system is designed at the operating point shown in Fig.2. The design parameters of the A2DOF current control system have been determined as

$$H_1 = -0.8 \; H_2 = n_{1i} = -0.9998 \; H_3 = -0.2 \; k_{zi} = 0.3 \tag{16}$$

Here since n_{2i} is very large, it can be disregarded. Then the current controller parameters become as

$$\begin{aligned} &k_1 = -0.0144013 \quad k_2 = 0.000699749 \\ &k_3 = 0.192984 \quad\;\; k_i = 0.00283157 \\ &k_{ri} = 0.00943857 \end{aligned} \tag{17}$$

And the parameters of the PI voltage controller have

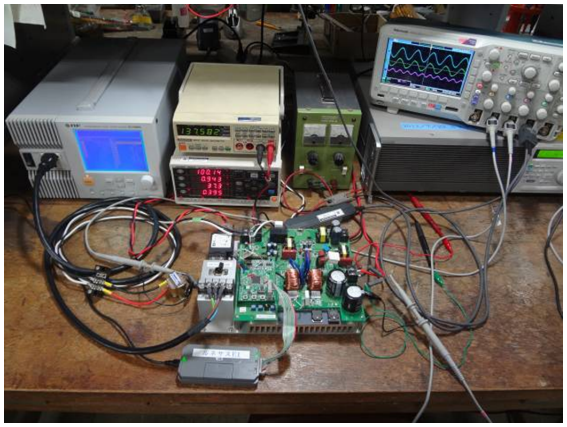

Fig.9: *Experimental setup system.*

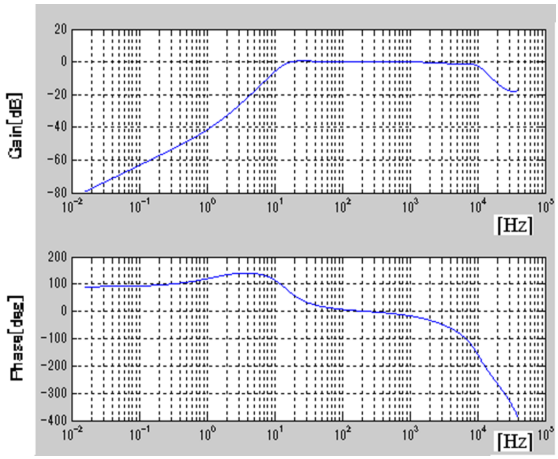

Fig.10: *The gain and phase characteristics of the current control system.*

been determined as

$$k_{rv} = 8 \quad k_{iv} = 0.01 \tag{18}$$

From these parameters the gain and phase characteristics of the current control system is shown in Fig.10. The control bandwidth about 10kHz is attained. The gain and phase characteristics of the voltage control system is shown in Fig.11. The control bandwidth about 25Hz is attained. The transfer function of the lead-lag controller is as follows:

$$G_z(z) = \frac{a_{10} + a11z^{-1}}{1 - b_{11}z^{-1}} \cdot \frac{a_{20} + a_{21}z^{-1}}{1 - b_{21}z^{-1}} \cdot K_c \tag{19}$$

The parameters of the current controller are determined as

$$\begin{aligned} a_{10} &= 0.008447 \quad a_{11} = -0.004863 \\ b_{11} &= 0.9964 \quad\;\; a_{20} = 1.089 \\ a_{21} &= -0.5136 \quad b_{21} = 0.4246 \\ K_c &= 60 \end{aligned} \tag{20}$$

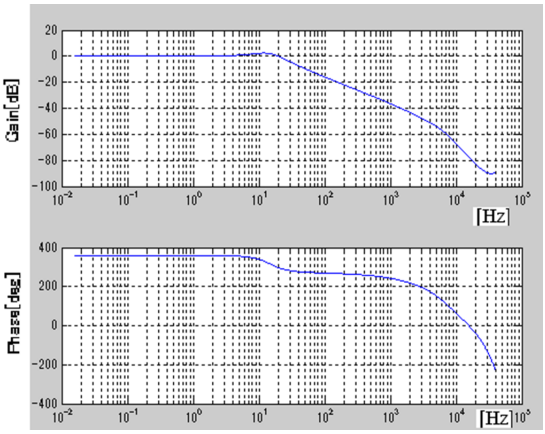

Fig.11: *The gain and phase characteristics of the voltage control system.*

The parameters of the voltage controller are determined as

$$\begin{aligned} a_{10} &= 0.002509 \quad a_{11} = -0.002491 \\ b_{11} &= 0.9999 \quad\;\; a_{20} = 1.320 \\ a_{21} &= -1.083 \quad b_{21} = 0.7627 \\ K_c &= 100 \end{aligned} \tag{21}$$

The experiment results of the steady state at load RL=500Ω and RL=1kΩ using the proposed method are shown in Fig.12 and Fig.13, respectively. In Fig.12, the input current waveform and the phase are the almost same as the input voltage. Then the power factor is 0.993. The input current waveform in Fig.13 is not distorted so greatly compared with the one in Fig.12. It turns out that the current control system proposed is robust. The experiment result of load sudden change from 1kΩ to 500Ω using the proposed method is shown in Fig.14. In Fig.14, the output voltage variation in sudden load change is less than 5V (1.27%). The experiment results of the steady state at load RL=500Ω and RL=1kΩ using the phase lead-lag control method are shown in Fig. 15 and Fig.16, respectively. The power factor is 0.985 in Fig. 15 and the distortion at zero crossing is seen. Therefore the current in Fig.15 has more harmonics than the one in Fig.12. It turns out that the proposed method is better than the phase lead-lag method in the power factor. This is because the distortion at zero crossing is lost in the proposed method. The input current waveform in Fig.16 is distorted greatly and has become a triangular wave. It turns out that the current control system using the phase lead-lag method is not robust and there are many harmonics in the input current compared with the one in Fig.13. The experiment result of load sudden change from 1kΩ to 500Ω using the phase lead-lag control method is shown in Fig.17. In Fig. 17, the output voltage variation in sudden load change is less than 10V (2.53%) and the oscillation is seen. It turns out that the output voltage regulation of the proposed method is better than the

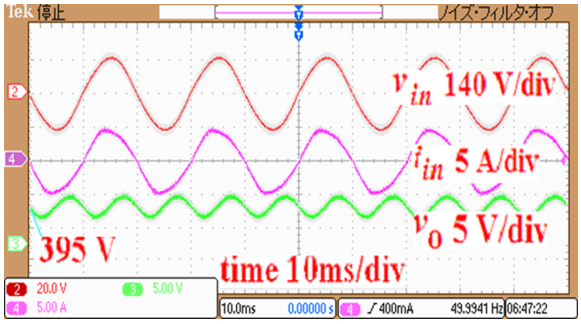

Fig.12: *Experimental result of steady state waveforms, at load RL=500Ω using the proposed method, PF=0.993.*

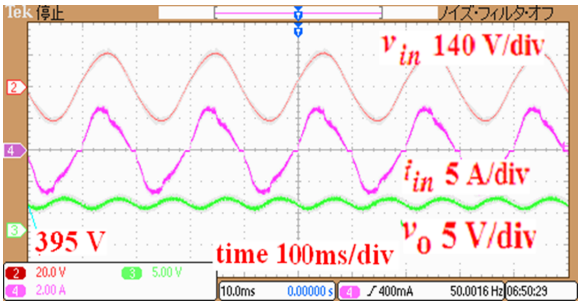

Fig.13: *Experimental result of steady state waveforms, at load RL=1kΩ using proposed method, PF=0.983.*

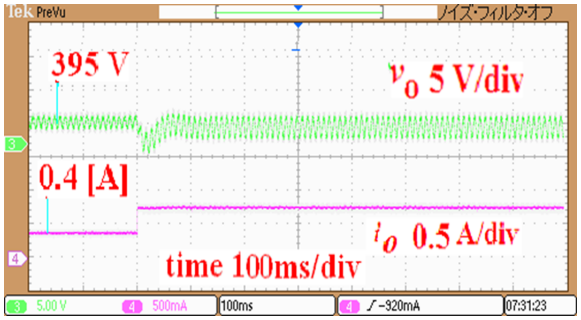

Fig.14: *Experimental result of sudden load change from 1kΩ to 500Ω using the proposed method.*

phase lead-lag control method. That is, the proposed controller is effective practically.

5. CONCLUSION

In this paper, the design method of robust controller for the interleaved boost converter combining the digital A2DOF current controller and the digital PI voltage controller was proposed. From experimental results, it was shown that the better characteristics of the power factor, the distortion and the output regulation were realizable by the proposed controller. A future subject is verifying the characteristic when the input voltage is changed.

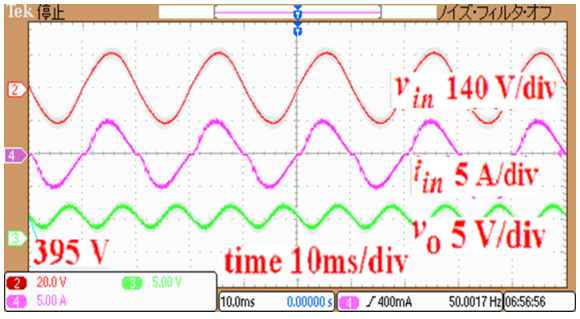

Fig.15: *Experimental result of steady state waveforms, at load RL=500Ω using the phase lead-lag method, PF=0.985.*

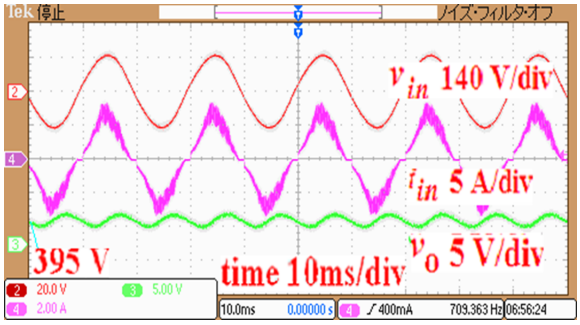

Fig.16: *Experimental result of steady state waveforms, at load RL=1kΩ using the phase lead-lag method, PF=0.978.*

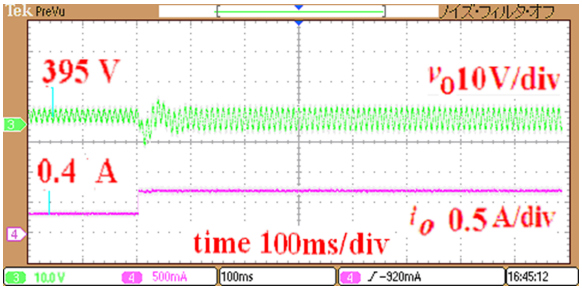

Fig.17: *Experimental result of sudden load change from 1kΩ to 500Ω using the phase lead-lag method.*

References

[1] L. Rossetto, G. Spiazzi, and P. Tenti, "Control techniques for power factor correction converters," *Proc. Power Electron. Motion Control*, 1994, pp.1310-1318.

[2] M. Xie, "Digital control for power factor correction," *Unpublished master's thesis*, Virginia Polytechnic Institute and State University, 2003.

[3] M. Fu and Q. Chen, "A DSP based controller for power factor correction (PFC) in a rectifier circuit," *IEEE Applied Power Electron. Conf. Exposition*, 2001, pp. 144-149.

[4] K. De Gusseme, D. M. Van de Sype, and J. A. A. Melkebeek, "Design issues for digital control of

boost power factor correction converters," *IEEE Int. Symp. Ind. Electron.*, 2002, pp.731-736.

[5] W. Zhang, G. Feng, Y. Liu, and B. Wu, "A digital power factor correction (PFC) control strategy optimized for DSP," *IEEE Trans. Power Electron.*, vol. 19, no. 6, pp.1474-1485, Nov. 2004.

[6] N. Genc, and I. Iskender, "DSP-based current sharing of average current controlled two-cell interleaved boost power factor correction converter", *IET Power Electron.*, vol. 4, no. 9, pp. 1015-1022, Nov. 2011.

[7] Y.-S. Kim, B.-K. Lee, and J. W. Lee, "Topology characteristics analysis and performance comparison for optimal design of high efficiency PFC circuit for telecom," *Proc. IEEE 33rd Int. Telecommun. Energy Conf.*, 2011, Oct. pp.1-7.

[8] M. Pahlevaninezhad, P. Das, J. Drobnik, G. Moschopoulos, P. K. Jain, and A. Bakhshai "A nonlinear optimal control approach based on the Control-Lyapunov Function for an AC/DC converter used in electric vehicles," *IEEE Trans. Ind. Informatics*, vol. 8, no. 3, pp. 596-614, Aug. 2012

[9] K. Higuchi, K. Nakano, T. Kajikawa, E. Takegami, S. Tomioka, and K. Watanabe, "A new design of robust digital controller for DC-DC converters," *IFAC 16th Triennial World Congress*, (CD-ROM), Jul. 2005.

[10] K. Higuchi, E. Takegami, K. Nakano, T. Kajikawa, and S. Tomioka, "Digital robust control for DC-DC converter with second-order characteristics," *Elect. Eng./Electron., Comput., Telecommun. Inform. Technology Conf.*, 2009, May. pp.161-169.

[11] Y. Ohta, K. Higuchi, and K. Chamnongthai, "Robust digital control for a PFC boost converter," *Elect. Eng./Electron., Comput., Telecommun. Inform. Technology Assoc. Trans. Elect. Eng., Elect., Commun.*, vol.10, no.2, pp. 164-172, Aug. 2012.

[12] Y. Ohta, and K. Higuchi, "Approximate 2-degree-of-freedom digital control for a PFC boost converter," *IEICE Electron. Express*, vol. 10, no. 10, pp.1-8 (20130152), May 2013.

[13] S. Sasaki, and H. Watanabe, "Analysis of multiple operating points for dynamical control of switching power converters," Inst. Electron., Inform. Commun. Eng. Tech. Rep., 2005, pp.33-38.

Yuto Adachi He is a master's course student in the first year of The University of Electro-Communications, Tokyo, Japan. He received his B. Eng. degree from The University of Electro-Communications, in 2012. His research interests include Power Electronics, Control Engineering, Digital Signal Processing and Embedded Systems Design.

Kohji Higuchi received his Ph.D. degree from Hokkaido University, Sapporo, Japan in 1981. In 1980 he joined the University of Electro-Communications, Tokyo, Japan, as an Research Associate, where he became an Assistant Professor in 1982 and currently an Associate Professor in the Dept. of Mechanical Engineering and Intelligent Systems, Electronic Control System Course. His interests include Power Electronics, Control Engineering and Digital Signal Processing. He is a member of IEEE, IEICE, SICE and IEEJ.

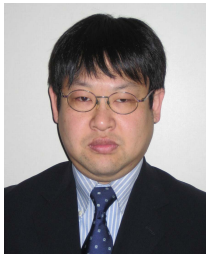

Tomoaki Sato received the B.S. and M.S. degrees from Hirosaki University, Japan, in 1996 and 1998 respectively, and the Ph.D. degree from Tohoku University, Japan, in 2001. From 2001 to 2005, he was an Assistant Professor of Sapporo Gakuin University, Japan. Since 2005, he has been an Associate Professor of Hirosaki University. And, he has been a Visiting Associate Professor of the Open University of Japan since 2012. His research interests include VLSI Design, Computer Hardware, Computer Architecture and Computer and Network Security.

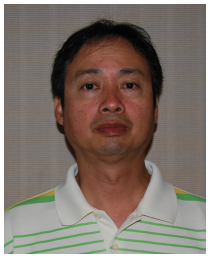

Kosin Chamnongthai currently works as associate professor at Electronic and Telecommunication Engineering Department, Faculty of Engineering, King Mongkut's University of Technology (KMUTT), and also serves as editor of ECTI e-magazine, and associate editor of ELEX (IEICE Trans) during 2008-2010 and ECTI-CIT Trans since 2011 until now. He served as assoc editor of ECTI-EEC Trans during 2003-2010, and chairman of IEEE COMSOC Thailand during 2004-2007. In organizing conference, he has served as general chair of international and national conferences such as SISA 2012, ITC-CSCC 2010, NICOGRAPH 2008, ISPACS 2008, ICESIT 2008, ICESIT 2007, IWAIT 2007, and 30th EECON.

He has recieved B.Eng. in Applied Electronics from the University of Electro-communications, Tokyo, Japan in 1985, M.Eng. in Electrical Engineering from Nippon Institute of Technology, Saitama, Japan in 1987 and D.Eng. in Electrical Engineering from Keio University, Tokyo, Japan in 1991. His research interests include image processing, computer vision, robot vision, and signal processing. He is a senior member of IEEE, and a member of IPS, TRS, IEICE, TESA and ECTI.